optica

Enhanced LIDAR performance metrics using continuous-wave photon-pair sources: supplementary material

HAN LIU[1], DANIEL GIOVANNINI[1], HAOYU HE[1], DUNCAN ENGLAND[2], BENJAMIN J. SUSSMAN[2,3], BHASHYAM BALAJI[4], AND AMR S. HELMY[1,*]

[1]*The Edward S. Rogers Department of Electrical and Computer Engineering, University of Toronto, 10 King's College Road, Toronto, Ontario M5S 3G4, Canada*

[2]*National Research Council of Canada, 100 Sussex Drive, Ottawa, Ontario, K1A 0R6, Canada*

[3]*Department of Physics, University of Ottawa, 598 King Edward, Ottawa, Ontario K1N 6N5, Canada*

[4]*Radar Sensing and Exploitation Section, Defense R&D Canada, Ottawa Research Centre, 3701 Carling Avenue, Ottawa, Ontario, K1A 0Z4, Canada*

[*]*a.helmy@utoronto.ca*

Published 10 October 2019

This document provides supplementary information to "Enhanced LIDAR performance metrics using continuous-wave photon-pair sources," https://doi.org/10.1364/OPTICA.6.001349.

1. DERIVATION OF SINGLES/COINCIDENCE COUNTING RATE

A. probe source and noise source

The SPDC state generated in the semiconductor waveguide could be expressed as:

$$|\Psi\rangle = |vac\rangle + \int_{-\infty}^{\infty}\int_{-\infty}^{\infty} \phi(t_p - t_r)\exp(-i\omega_{p,0}t_p - i\omega_{r,0}t_r) \, a_p^\dagger(t_p)a_r^\dagger(t_r)dt_p dt_r\,|vac\rangle \tag{S1}$$

where a_p, a_r are the waveguide mode operators that probe and reference photons are generated in. The density operator of the source is just $\rho_{pr} = |\Psi\rangle\langle\Psi|$. The generation flux of the probe and reference photon is:

$$\nu = \mathrm{tr}\{\rho_{pr}a_p^\dagger(t)a_p(t)\} = \int_{-\infty}^{+\infty} |\phi(t-t_r)|^2 dt_r \tag{S2}$$

where tr stand for the trace over the total Hilbert space. We assume that the background noise photons occupy a single mode a_b with density operator ρ_b. The flux $\nu_{b,0}$ of the noise photons is given by:

$$\nu_{b,0} = \mathrm{tr}\{\rho_b a_b^\dagger(t)a_b(t)\} \tag{S3}$$

B. POVM of the photon detection events

We first model the photon detection events on the detector x (with $x = p, r$ denoting the probe or reference detector, respectively). Since we are only interested in the rates of different photon detection events (single detector detection, coincidence detection and no detection), it suffices to consider a small time interval $\mathcal{T} = [t - \frac{\tau}{2}, t + \frac{\tau}{2})$ during which the photon detection probability is much less than unity. There are only two possible kinds of detection outcome for either detector $x = p, r$: no detection or detecting a single photon at time $t_x \in \mathcal{T}$. The no detection event is modeled by projection onto vacuum state of the mode x: $V_x = |vac_x\rangle\langle vac_x|$. To include the effect of the finite temporal resolution Δt of the detectors, we model the photon detection event at time t_x on detector x as the operator $\Pi_x(t_x)$:

$$\Pi_x(t_x) = \frac{1}{\Delta t}\int_{t_x-\frac{\Delta t}{2}}^{t_x+\frac{\Delta t}{2}} b_x^\dagger(t')b_x(t')dt' \tag{S4}$$

where the mode operator b_x denote the detected mode of detector x. We model the inefficiency of the detector as the loss from the waveguide mode a_x to the detected mode b_x so that the detection efficiency on mode b_x could be treated as 100%. The Δt characterizes the temporal resolution of the detectors. $\{\Pi_x(t_x)\}_{t_x\in\mathcal{T}}$ altogether with V_x forms a POVM on the sub Hilbert space of the photon in mode x, provided that the total photon number in mode x over time $\mathcal{T}$ is not more than than one:

$$\int_{t_x\in\mathcal{T}} \Pi_x(t_x)dt_x + V_x = \mathcal{I}_x \tag{S5}$$

where $\mathcal{I}_x$ stand for the identity operator on mode x. The total POVM corresponding to the joint photon detection event (single detector detection, coincidence detection and no detection) is just a tensor product of the two single detector POVMs ($x = p$ and $x = r$) :

$$V_p \otimes V_r + \int_{t_r \in \mathcal{T}} dt_r V_p \otimes \Pi_r(t_r) + \int_{t_p \in \mathcal{T}} dt_p \Pi_p(t_p) \otimes V_r + \iint_{t_p, t_r \in \mathcal{T}} dt_p dt_r \Pi_p(t_p) \otimes \Pi_r(t_r) = \mathcal{I} \tag{S6}$$

where $\mathcal{I}$ is the identity operator on the joint Hilbert space. The four terms in the above expression correspond to (from left to right) no detection on either detector, only probe detector fires at time t_p, only reference detector fires at t_r, and both detector fire at (t_p, t_r).

C. singles counting rate

We shall work in the Heisenberg picture. Denote the joint quantum system as $\rho_d = \rho_{pr} \otimes \rho_b \otimes \rho_v$. Here the vacuum density operator ρ_v is on a mode that is used to model the attenuation of the reference photons. Then the total number of photon detected at detector $x = p, r$ over the interval $\mathcal{T}$ is given by:

$$\begin{aligned} \langle N_x \rangle &= \int_{t-\frac{\tau}{2}}^{t+\frac{\tau}{2}} dt_x tr\{\Pi_x(t_x)\rho_d\} \\ &= \int_{t-\frac{\tau}{2}}^{t+\frac{\tau}{2}} dt_x \int_{t_x-\frac{\Delta t}{2}}^{t_x+\frac{\Delta t}{2}} dt' tr\{b_x^\dagger(t')b_x(t')\rho_d\} \end{aligned} \tag{S7}$$

The expression Eq. (S7) could be evaluated through expanding the detector mode operators b_x to the waveguide mode operator a_x. We model the loss of the reference channel as the mixing between the waveguide mode for the reference photons a_r and the vacuum mode a_v at a balanced beam-splitter with transmission η_r for the reference photon. Similarly, we model the noise and loss in the probe channel as the mixing between the waveguide mode a_p and the background noise mode a_b at a beam-splitter with transmission η_p for the probe photon. Through operator expansion, the detected mode operator $b_p(b_r)$ could be expressed in terms of waveguide mode operators $a_p(a_r)$ and the background noise mode operator a_b (and the vacuum mode operator a_v):

$$\begin{bmatrix} b_r \\ b_{r'} \end{bmatrix} = \begin{bmatrix} \sqrt{\eta_r} & i\sqrt{1-\eta_r} \\ i\sqrt{1-\eta_r} & \sqrt{\eta_r} \end{bmatrix} \begin{bmatrix} a_r \\ a_v \end{bmatrix} \tag{S8}$$

$$\begin{bmatrix} b_p \\ b_{p'} \end{bmatrix} = \begin{bmatrix} \sqrt{\eta_p} & i\sqrt{1-\eta_p} \\ i\sqrt{1-\eta_p} & \sqrt{\eta_p} \end{bmatrix} \begin{bmatrix} a_p \\ a_b \end{bmatrix} \tag{S9}$$

where b'_r, b'_p are the mode operators of the "unused output port ports" of the virtual beam-splitters. Then the photon detection rate Eq. (S7) on the probe detector ($x = p$) could be expressed in terms of the generated SPDC state $\rho_{pr} = |\Psi\rangle\langle\Psi|$ and the density operator of the background noise mode ρ_b:

$$\langle N_p \rangle = \int_{t-\frac{\tau}{2}}^{t+\frac{\tau}{2}} dt_x \int_{t_x-\frac{\Delta t}{2}}^{t_x+\frac{\Delta t}{2}} dt' tr\{b_p^\dagger(t')b_p(t')\rho_d\} \tag{S10}$$

$$= \int_{t-\frac{\tau}{2}}^{t+\frac{\tau}{2}} dt_x \int_{t_x-\frac{\Delta t}{2}}^{t_x+\frac{\Delta t}{2}} dt' (\eta_p tr\{a_p^\dagger(t')a_p(t')\rho_{pr} \otimes \rho_b\} \tag{S11}$$

$$+(1-\eta_p)tr\{a_b^\dagger(t')a_b(t')\rho_{pr} \otimes \rho_b\}$$

$$+i\sqrt{\eta_p(1-\eta_p)}tr\{a_p^\dagger(t')a_b(t')\rho_{pr} \otimes \rho_b\} \tag{S12}$$

$$-i\sqrt{\eta_p(1-\eta_p)}tr\{a_b^\dagger(t')a_p(t')\rho_{pr} \otimes \rho_b\}) \tag{S13}$$

$$= \int_{t-\frac{\tau}{2}}^{t+\frac{\tau}{2}} dt_x \int_{t_x-\frac{\Delta t}{2}}^{t_x+\frac{\Delta t}{2}} dt' (\eta_p \mathrm{tr}\{a_p^\dagger(t')a_p(t')\rho_{pr}\} \tag{S14}$$

$$+(1-\eta_p)\mathrm{tr}\{a_b^\dagger(t')a_b(t')\rho_b\}$$

$$+i\sqrt{\eta_p(1-\eta_p)}\mathrm{tr}\{a_p^\dagger(t')\rho_{pr}\}\mathrm{tr}\{a_b(t')\rho_b\} \tag{S15}$$

$$-i\sqrt{\eta_p(1-\eta_p)}\mathrm{tr}\{a_p(t')\rho_{pr}\}\mathrm{tr}\{a_b^\dagger(t')\rho_b\}) \tag{S16}$$

The last two terms are vanishing because the probe photons have zero average phase $\mathrm{tr}\{a_p(t)\rho_{pr}\} = 0, \mathrm{tr}\{a_p^\dagger(t)\rho_{pr}\} = 0$. By definition the probe photon flux $\nu = \mathrm{tr}\{a_p^\dagger(t')a_p(t')\rho_{pr}\} = \int_{-\infty}^{+\infty} |\phi(t'-t_r)|^2 dt_r$ and $\nu_{b,0} = \mathrm{tr}\{a_b^\dagger(t')a_b(t')\rho_b\}$ is the generation flux of the probe photons and the noise photons. Then the photon-detection rate P_p^* on the probe detector could be expressed as:

$$P_p^* = \frac{\langle N_p \rangle}{\tau} = \eta_p \nu + (1-\eta_p)\nu_{b,0} \tag{S17}$$

Similarly, the photon-detection rate on the reference detector P_r^* could be expressed as:

$$P_r^* = \frac{\langle N_r \rangle}{\tau} = \eta_r \nu \tag{S18}$$

The single channel detection rates P_p, P_r are defined as the rate of the photon detection events that does not contribute to coincidence detection:

$$P_p = P_p^* - P_c \tag{S19}$$

$$P_r = P_r^* - P_c \tag{S20}$$

where P_c is the coincidence detection rate that will be defined in the next section.

D. coincidence counting rate

Now we consider the coincidence detection events that are contributed by both detectors for the small time interval $\mathcal{T}$. The probability density of detecting one photon on the probe detector at time $t_p \in \mathcal{T}$ and detecting one photon on the reference detector at time $t_r \in \mathcal{T}$ is given by $p(t_p, t_r) = tr\{\Pi_p(t_p)\Pi_r(t_r)\rho_d\}$.

Again through operator expansion, it could be shown that:

$$\Pi_p(t_p)\Pi_r(t_r) = \frac{1}{\Delta t^2}\int_{t_p-\frac{\Delta t}{2}}^{t_p+\frac{\Delta t}{2}}\int_{t_r-\frac{\Delta t}{2}}^{t_r+\frac{\Delta t}{2}} b_p^\dagger(t_p')b_p(t_p')b_r^\dagger(t_r')b_r(t_r')dt_p'dt_r' \tag{S21}$$

$$= \frac{1}{\Delta t^2}\int_{t_p-\frac{\Delta t}{2}}^{t_p+\frac{\Delta t}{2}}\int_{t_r-\frac{\Delta t}{2}}^{t_r+\frac{\Delta t}{2}} dt_p'dt_r' \tag{S22}$$

$$\{\eta_p a_p^\dagger(t_p')a_p(t_p') + (1-\eta_p)a_b^\dagger(t_p')a_b(t_p') \tag{S23}$$

$$+i\sqrt{\eta_p(1-\eta_p)}(a_p^\dagger(t_p')a_b(t_p') - a_p(t_p')a_b^\dagger(t_p'))\} \tag{S24}$$

$$\times\{\eta_r a_r^\dagger(t_r')a_r(t_r') + (1-\eta_r)a_v^\dagger(t_r')a_v(t_r') \tag{S25}$$

$$+i\sqrt{\eta_r(1-\eta_r)}(a_r^\dagger(t_r')a_v(t_r') - a_r(t_r')a_v^\dagger(t_r'))\} \tag{S26}$$

Simple calculation shows that Eq. (S24), and Eq. (S26) do not contribute to coincidence detection events for the joint state ρ_d. Then the probability $p(t_r, t_b)$ of detecting one photon on the probe detector at time t_p and detecting one photon on the reference detector at time t_r is given by:

$$p(t_p, t_r) = tr\{\rho_d \Pi_p(t_p)\Pi_r(t_r)\} \tag{S27}$$

$$= \frac{1}{\Delta t^2}\int_{t_p-\frac{\Delta t}{2}}^{t_p+\frac{\Delta t}{2}}\int_{t_r-\frac{\Delta t}{2}}^{t_r+\frac{\Delta t}{2}} dt_p'dt_r' \tag{S28}$$

$$tr\{\rho_{pr}\otimes\rho_b\{\eta_p a_p^\dagger(t_p')a_p(t_p') + (1-\eta_p)a_b^\dagger(t_p')a_b(t_p')\} \tag{S29}$$

$$\times\{\eta_r a_r^\dagger(t_r')a_r(t_r') + (1-\eta_r)a_v^\dagger(t_r')a_v(t_r')\}\} \tag{S30}$$

$$= \frac{1}{\Delta t^2}\int_{t_p-\frac{\Delta t}{2}}^{t_p+\frac{\Delta t}{2}}\int_{t_r-\frac{\Delta t}{2}}^{t_r+\frac{\Delta t}{2}} dt_p'dt_r'\{(1-\eta_p)\eta_r\nu_b\nu + \eta_p\eta_r|\phi(t_p'-t_r')|^2\} \tag{S31}$$

$$= (1-\eta_p)\eta_r\nu_b\nu + \frac{\eta_p\eta_r}{\Delta t^2}\int_{t_p-\frac{\Delta t}{2}}^{t_p+\frac{\Delta t}{2}}\int_{t_r-\frac{\Delta t}{2}}^{t_r+\frac{\Delta t}{2}} dt_p'dt_r'|\phi(t_p'-t_r')|^2 \tag{S32}$$

The first term is the contribution of noise-reference photon pairs to coincidence detection events. The contribution of actual probe-reference photon pairs to $p(t_p, t_r)$ is given by:

$$p_{pairs}(t_p, t_r) = \frac{\eta_p\eta_r}{\Delta t^2}\int_{t_p-\frac{\Delta t}{2}}^{t_p+\frac{\Delta t}{2}}\int_{t_r-\frac{\Delta t}{2}}^{t_r+\frac{\Delta t}{2}} dt_p'dt_r'|\phi(t_p'-t_r')|^2 \tag{S33}$$

$$= \frac{\eta_p\eta_r}{\Delta t^2}\int_{-\infty}^{+\infty}\int_{-\infty}^{+\infty} dt''dt\mathrm{Gate}(\frac{t-t_p+t''}{\Delta t})\mathrm{Gate}(\frac{t-t_r}{\Delta t})dt|\phi(t'')|^2 \tag{S34}$$

$$= \frac{\eta_p\eta_r}{\Delta t}\int dt''\mathrm{tri}(\frac{t_p-t_r-t''}{\Delta t})|\phi(t'')|^2 \tag{S35}$$

where Gate(t) is is one over $[-1/2, 1/2]$ and zero otherwise. Triangle function tri(x) is the convolution between two gate function Gate(t). From the above equation it could be seen that $p_{pairs}(t_p, t_r)$ is the convolution of the triangle function tri$(\frac{t_p-t_r-t''}{\Delta t})$ (dictated by the detector temporal resolution Δt) and the temporal correlation function $|\phi(t'')|^2$ (related to the joint temporal intensity function $|\phi(t_p - t_r)|^2$).

During the interval $\mathcal{T}$, the average number of coincidence detections $\langle N_c\rangle$ is related to the coincidence window T_c:

$$\langle N_c\rangle = \int_{t-\frac{\tau}{2}}^{t+\frac{\tau}{2}} dt_p\int_{t_p-\frac{T_c}{2}}^{t_p+\frac{T_c}{2}} dt_r p(t_p, t_r) \tag{S36}$$

$$= 2(1-\eta_p)\eta_r\nu_b\nu\tau T_c + \int_{t-\frac{\tau}{2}}^{t+\frac{\tau}{2}} dt_p\int_{t_p-T_c/2}^{t_p+T_c/2} dt_r p_{pairs}(t_p, t_r) \tag{S37}$$

The second term of the above equation represents the number of coincidence detection events that are due to actual SPDC photon pairs. To ensure that each probe-reference photon pair detected will contribute to a coincidence detection event, the coincidence window T_c must exceeds the sum of the full width of the triangle function tri$(\frac{t_p-t_r-t''}{\Delta t})$ and the temporal correlation function $|\phi(t'')|^2$. The full width of the triangle function is twice the detector temporal resolution Δt and the full width of the temporal correlation function is given by 3 times the intrinsic correlation time Δt_0. We defined the effective temporal correlation time Δt_{eff} as:

$$\Delta t_{eff} = 2\Delta t + 3\Delta t_0 \tag{S38}$$

When $T_c \geq \Delta t_{eff}$, the integral in Eq. (S37) could be approximated by $\eta_p\eta_r\nu$ and the coincidence detection rate is given by:

$$P_c = \frac{\langle N_c\rangle}{\tau} = (1-\eta_p)\eta_r\nu_{b,0}\nu T_c + \eta_p\eta_r\nu \tag{S39}$$

Note that in the above expression P_c for the coincidence counting rate, the contribution of accidental coincidence detection events is neglected (an accidental coincidence detection event is contributed by a probe and a reference photon from two different photon pairs). This approximation is valid in our experiment because the coincidence detection window $T_c \simeq 200$ps is much less than the average interval of the photon pair generation $1/3.87$MHz $\simeq 258$ns.

E. correction of the beam-splitter model

We adopt a hypothetical beam-splitter with transmission η_p to model the total transmission of the probe photons and the mixing of the probe photons and noise photons. However, this simple model has a big problem: the detected noise power is dependent on the probe photon transmission η_p. Therefore to ensure constant noise flux ν_b detected on the probe detector regardless of the probe transmission η_p, we set the noise source flux:

$$\nu_{b,0} = \nu_b/(1-\eta_p) \tag{S40}$$

Then the single channel detection rate P_p, P_r and the coincidence detection rate P_c (with $T_c = \Delta t_0$) could be rewritten as:

$$P_p = \eta_p\nu + \nu_b - P_c \tag{S41}$$

$$P_r = \eta_r\nu - P_c \tag{S42}$$

$$P_c = \frac{\langle N_c\rangle}{\tau} = \eta_r\nu_b\nu T_c + \eta_p\eta_r\nu \tag{S43}$$

2. DEPENDENCE OF THE FISHER INFORMATION ON DIFFERENT EXPERIMENTAL PARAMETERS

In this section, we study the ratio of the total Fisher information I_{CDNC}/I_{CDC} (the Fisher information for the CDNC scheme over the Fisher information for the CDC scheme) as a function of the experimental parameters of target detection systems. The analytical expression of I_{CDNC} is given below. The expression of I_{CDC} is the same as I_{CDNC} except for the CDC scheme η_r is always zero.

$$I_{CDNC} = \frac{\eta_r^2\nu^2\tau}{P_c} + \frac{(1-\eta_r)^2\nu^2\tau}{P_p} + \frac{\eta_r^2\nu^2\tau}{P_r} \tag{S44}$$

$$I_{CDC} = \frac{\nu^2\tau}{P_p} \tag{S45}$$

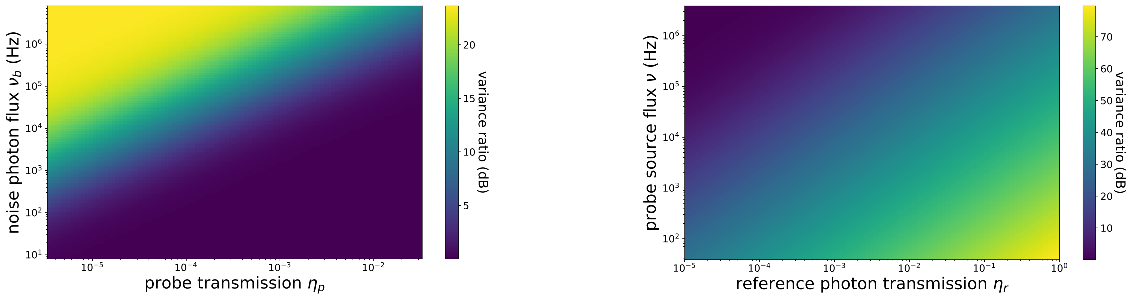

Fig. S1. Left: Fisher information ratio between the CDNC scheme and the CDC scheme as a function of probe photon transmission η_p and detected noise flux ν_b. The reference photon transmission η_r and probe source flux is taken to be 17.8% and 3.87MHz. Right: Fisher information ratio as a function of reference photon transmission η_r and source photon flux ν. The probe photon transmission η_p and detected noise flux ν_b is taken to be 3.87×10^{-5} and 0.4MHz.

The Fisher information ratio I_{CDNC}/I_{CDC} as a function of the probe source flux η_p, noise photon flux ν_b, probe photon transmission η_p and reference photon transmission η_r is shown in figure(S1). The coincidence window T_c in both plots is taken to be 200ps. As could be seen, the maximal enhancement is achieved in low probe transmission η_p, hight noise ν_b regime, highlighting the performance advantages of the CDNC scheme in lossy and noisy environment. The ratio also increases as the reference photon transmission η_r increase and the probe generation flux ν decrease.

3. SPDC PHOTON PAIR BANDWIDTH ESTIMATION

A joint spectral intensity measurement was performed to estimate the bandwidth of SPDC photons, shown in Fig(S2). Each photon is coupled into a 5km dispersive fiber, connected to a single photon detector. Since light with difference frequencies travels at different speeds in the fiber, due to dispersion, the frequency of each individual photon can be calculated from the detection time at the single photon detector[1]. The 80MHz laser trigger is used as a fixed time reference. Fig. S2(b) shows the joint spectral intensity measurement result. The SPDC bandwidth is estimated to be more than 100nm.

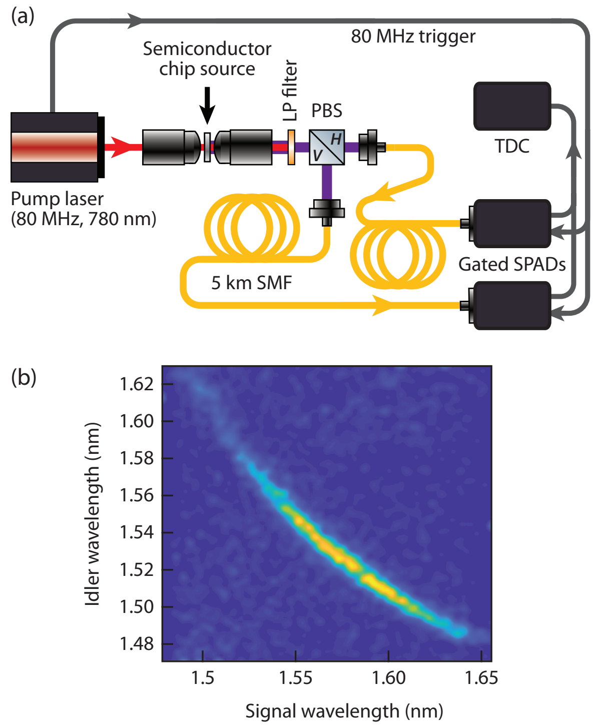

Fig. S2. (a) Diagrammatic representation of the experimental setup for joint spectral intensity measurements. LP: long-pass; SMF: single-mode fiber; SPAD: single-photon avalanche diode; TDC: time-to-digital converter. (b) Joint spectral intensity result.

4. COMPARISON BETWEEN CDNC AND PULSED CDC SCHEME

In this section the performance of the CDC scheme with pulsed probe light will be compared to the CDNC scheme with the same average probe flux ν, average detected noise flux ν_b and detector temporal resolution Δt. For a CDNC scheme, the Fisher information I_{CDNC} is given by:

$$I_{CDNC} = I(\nu, \nu_b, \eta_p, \eta_r, T_c, \tau) \tag{S46}$$

where $T_c = \Delta t_{eff} \simeq 2\Delta t$ is taken to be the effective temporal resolution. Then:

$$I(\nu, \nu_b, \eta_p, \eta_r, T_c, \tau) = \left(\frac{\eta_r^2 \nu^2}{P_c} + \frac{(1-\eta_r)^2\nu^2}{P_p} + \frac{\eta_r^2\nu^2}{P_r}\right)\tau \tag{S47}$$

For a CDC scheme with pulsed probe photon and gated detection, it suffices to consider the set of the time intervals when the gated detector is turned on. In the limit of pulse duration being much shorter than the detector temporal resolution Δt the gated detection window could be taken as Δt. Then the total detection time in the CDC scheme is just $\tau_{CDC} = f_{rep}\tau\Delta t$ where f_{rep} is the repetition rate of the probe pulses. It is obvious that such pulsed CDC scheme is equivalent to a CDC scheme with CW probe light but over shorter time τ_{CDC} and with a higher mean probe flux $\nu_{CDC} = \frac{\tau}{\tau_{CDC}}\nu$. Then the old analysis of the CDC scheme applies. The Fisher information $I_{CDC,pulsed}$ is given by:

$$I_{CDC,pulsed} = I(\nu_{CDC}, \nu_b, \eta_p, 0, 0, \tau_{CDC}) \tag{S48}$$

Figure (S3) shows the comparison between the performance of the CDNC and pulsed CDC scheme in terms of the estimation variance of the probe transmission η_p (the inverse of the Fisher information). It could be seen that if the repetition rate f_{rep}

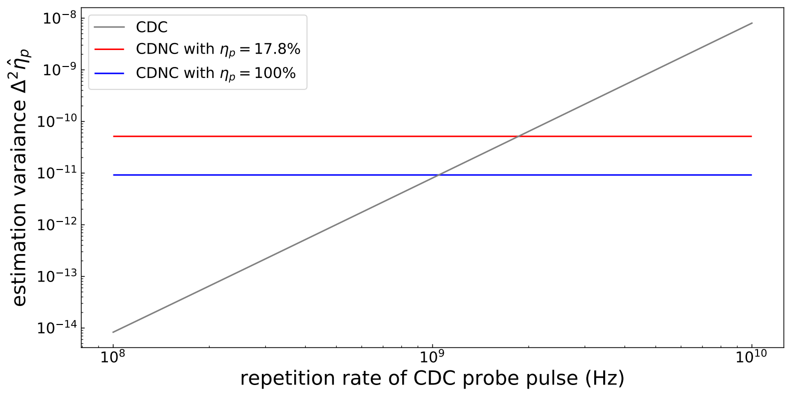

Fig. S3. Estimation variance of the pulsed CDC scheme (grey line) as a function of the probe pulse repetition rate. The probe photon transmission is $\eta_p = 3.3 \times 10^{-5}$. The average probe flux and noise flux are given by $\nu = 3.87$MHz and $\nu_b = 0.4$MHz. The red and blue lines correspond to the CDNC scheme performance with reference photon transmission $\eta_r = 17.8\%$ and $\eta_r = 100\%$. The detector temporal resolution of both the CDNC and the CDC scheme is taken to be 100ps.

of the pulsed probe light is lower than a certain value, which corresponds to a certain level of peak power, the pulsed CDC scheme could perform better than the CDNC scheme.

5. AN EXAMPLE OF IMPROVED PHOTON DETECTION TECHNIQUES: ENHANCING THE MEASURABLE TEMPORAL CORRELATION WITH DISPERSION CANCELLATION

In this section, we present an example of improved photon detection techniques that can fully exploit the strong temporal correlation of the SPDC photon pairs, without improving the detector temporal resolution, to benefit practical target detection protocols. The basic idea of this technique is inspired by the non-local dispersion cancellation [2] and the schematic of the experimental setup is shown in Fig. S4. The CW probe light (collected with the telescope) and reference light are divided into multiple pairs of probe-reference channels. In each pair of the channels the probe light and the reference light could be considered as pulsed. The duration of the pulses depends on the parameters of the time-division multiplexer (TDM). The reference and probe photon will go through chromatic dispersion of equal amount but opposite sign, before getting detected upon the single photon detectors. The detectors have limited temporal resolution $\Delta t = 50$ps.

In this proof-of-principle example, we will focus on quantifying the measurable temporal correlation between the probe and reference photon in each channel pair. Therefore for the conciseness of the analysis, the effect of the environmental noise and loss is neglected. We further assume that before arriving at the TDM, the probe and reference photons have traveled the same optical distance, therefore a pair of probe and reference photons will not be separated by the TDM (this condition is not necessary for a physical implementation but it will help simplify the analysis). Under these assumptions, the joint state of the pulsed probe-reference photon pair in each probe-reference channel pair (before going through the chromatic dispersion) could be described as:

$$|\text{pulsed pair}\rangle = \int\int f(t_p, t_r) \exp(-i\omega_0 t_p - i\omega_0 t_r) a_p^\dagger(t_p) a_r^\dagger(t_r) dt_p dt_r \tag{S49}$$

where $a_p^\dagger(t_p), a_r^\dagger(t_r)$ is the creation operator of the probe and the reference photon at time t_p, t_r. The central frequency of both photon are ω_0. The joint temporal amplitude $f(t_p, t_r)$ is assumed to be Gaussian for simplicity of the analysis:

$$f(t_p, t_r) = C \exp(-\frac{(t_p + t_r)^2}{8\sigma_+^2} - \frac{(t_p - t_r)^2}{8\sigma_-^2}) \tag{S50}$$

where σ_+ and σ_- characterize the pulse duration and the mean detection time difference (proportional to Δt_0) between the probe and reference photons. The constant C is to ensure that f is square normalized. The joint temporal amplitude $f_{dispersd}(t_p, t_r)$ after applying opposite chromatic dispersion to the probe and the reference photons is given by:

$$f_{dispersed}(t_p, t_r) = \mathcal{F}^{-1}\{\exp(\frac{i}{2}\beta^{(2)} l \omega_p^2 - \frac{i}{2}\beta^{(2)} l \omega_r^2)\mathcal{F}[f(t_p, t_r)]\} \tag{S51}$$

$$= C \exp((2\left(\sigma_+^2 - \sigma_-^2\right) t_r t_p + \left(2i\beta^{(2)} l - \sigma_-^2 - \sigma_+^2\right) t_r^2 \tag{S52}$$

$$+ \left(-2i\beta^{(2)} l - \sigma_-^2 - \sigma_+^2\right) t_p^2)/(8\left((\beta^{(2)} l)^2 + \sigma_-^2\sigma_+^2\right))) \tag{S53}$$

where $\beta^{(2)}$ is the group velocity dispersion and l is the length of the dispersive medium. The $\mathcal{F}$ and $\mathcal{F}^{-1}$ stand for the two dimensional Fourier and inverse Fourier transform between t_p, t_r and ω_p, ω_r. The joint temporal distribution JTI of the probe-reference photon detection time is given by the mod-square of $f_{dispersed}$:

$$\text{JTI} = |f_{dispersed}|^2 \tag{S54}$$

$$= |C|^2 \exp(-\frac{(t_p + t_r)^2}{4(\frac{(\beta^{(2)} l)^2}{\sigma_-^2} + \sigma_+^2)} - \frac{(t_p - t_r)^2}{4(\frac{(\beta^{(2)} l)^2}{\sigma_+^2} + \sigma_-^2)}) \tag{S55}$$

The experimentally detected joint temporal distribution JTI_{det} is a convolution between JTI and detector temporal response $g(t_p)$

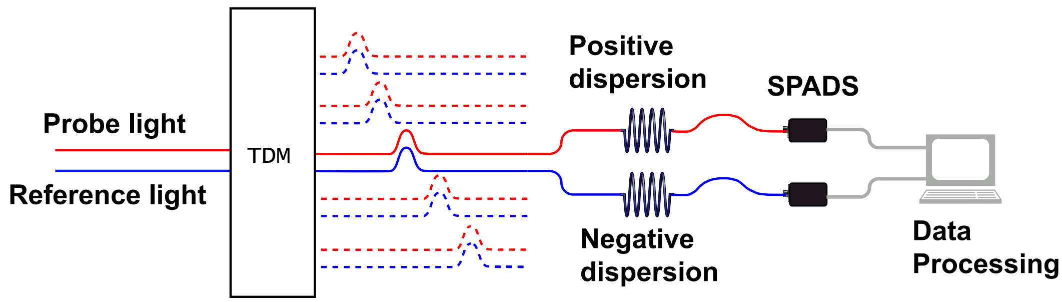

Fig. S4. the schematic of the enhanced detection technique. TDM: time division multiplexer. SPADS: single photon avalanche diodes.

and $g(t_r)$:

$$g(t) = \frac{1}{\sqrt{2\pi}\sigma_d}\exp(-\frac{t^2}{2\sigma_d^2}) \tag{S56}$$

where σ_d characterize the temporal resolution of both the probe and the reference detectors. Then:

$$\mathrm{JTI}_{det} = |C|^2\exp\left(-\frac{(t_p+t_r)^2}{4(\frac{(\beta^{(2)}l)^2}{\sigma_-^2}+\sigma_+^2+\sigma_d^2)} - \frac{(t_p-t_r)^2}{4(\frac{(\beta^{(2)}l)^2}{\sigma_+^2}+\sigma_-^2+\sigma_d^2)}\right) \tag{S57}$$

With realistic experimental parameters, the simulated JTI_{det} with dispersion $\beta^{(2)}l \neq 0$ and without dispersion $\beta^{(2)}l = 0$ is shown in Fig. S5. As could be seen, introducing additional chromatic dispersion could significantly increase the measurable temporal correlation between the probe and the reference photon. This is because the chromatic dispersion will broaden the individual pulse shape of both the reference and the probe photon and hence the stretch the joint probability distribution JTI_{det} to a much wider extent. Then the effect of the detector time uncertainty could be effectively minimized.

The temporal correlation measured from JTI_{det} could be quantified in terms of the variance and the covariance between the probe and reference photon detection time t_p, t_r [3]:

$$\rho_{t_p,t_r} = \frac{\mathrm{Cov}(t_p,t_r)}{\sqrt{\mathrm{var}(t_p)\mathrm{var}(t_r)}} = \frac{(\frac{(\beta^{(2)}l)^2}{\sigma_+^2\sigma_-^2}+1)(\sigma_+^2-\sigma_-^2)}{(\frac{(\beta^{(2)}l)^2}{\sigma_+^2\sigma_-^2}+1)(\sigma_+^2+\sigma_-^2)+2\sigma_d^2} \tag{S58}$$

The dependence of the measured correlation ρ_{t_p,t_r} on the amount of chromatic dispersion is plotted in Fig. S5. The effective temporal resolution is defined as the temporal resolution that is required to achieve the same amount of measurable temporal correlation without applying any dispersion. As could be seen in Fig. S5, the improved detection technique could drastically increase the measurable temporal correlation and decrease the effective temporal resolution from 50ps to around 500fs. It worth noting that if the detector temporal resolution is perfect ($\sigma_d = 0$), the temporal correlation ρ_{t_p,t_r} is not affected by the chromatic dispersion, as could be seen in equation Eq. (S58).

REFERENCES

1. E. Y. Zhu, C. Corbari, P. G. Kazansky, and L. Qian, "Self-calibrating fiber spectrometer for the measurement of broadband downconverted photon pairs," (2015). ArXiv:1505.01226 [quant-ph].
2. J. Franson, "Nonlocal cancellation of dispersion," Phys. Rev. A **45**, 3126 (1992).
3. M. H. DeGroot and M. J. Schervish, *Probability and statistics* (Pearson Education, 2012).

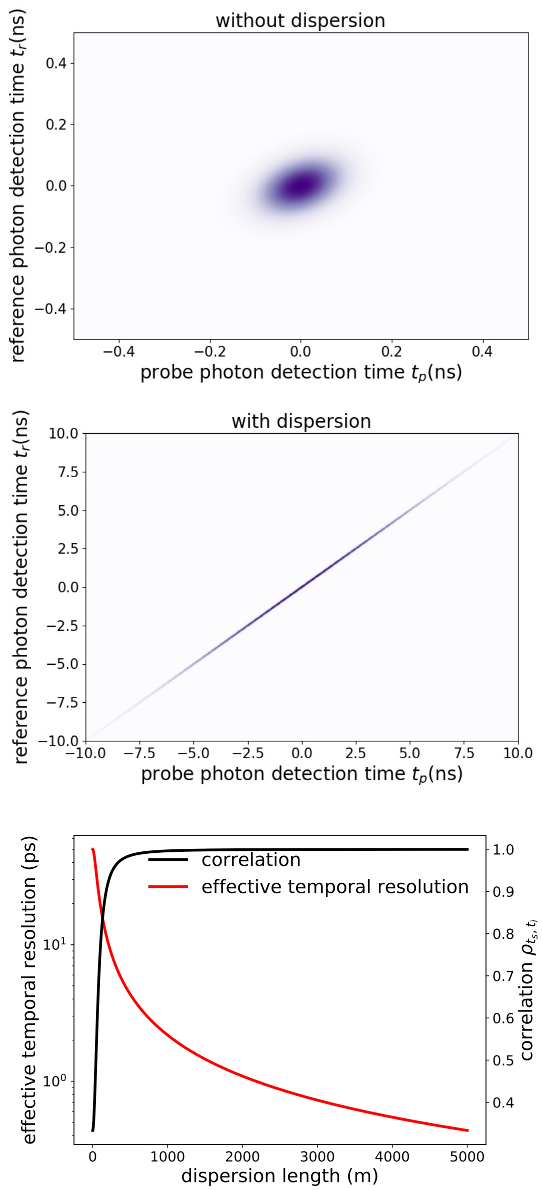

Fig. S5. Top: simulated joint temporal amplitude JTI_{det} with dispersion (right, $\beta^{(2)}l = 1.147 \times 10^{-22}s^2$) and without dispersion (left, $\beta^{(2)}l = 0$). Detector temporal resolution $\sigma_d = 50$ps, detection time difference (without dispersion): $\sigma_- = 20$fs, probe and reference pulse duration $\sigma_+ = 50ps$. Bottom: the dependence between the dispersion length ($\beta^{(2)} = 2.294 \times 10^{-26}s^2/m$) and the temporal correlation and the effective temporal resolution. Other parameters are the same as the top plot.